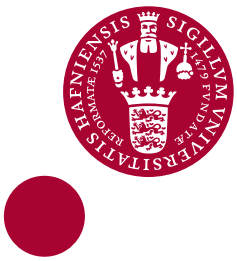

An automated microfluidic device for time-lapse imaging of mouse embryonic stem cells

Laing, Adam F; Tirumala, Venkat; Hegarty, Evan; Mondal, Sudip; Zhao, Peisen; Hamilton, William B; Brickman, Joshua M; Ben-Yakar, Adela

Published in:
Biomicrofluidics

DOI:
10.1063/1.5124057

Publication date:
2019

Document version
Publisher's PDF, also known as Version of record

Biomicrofluidics ARTICLE scitation.org/journal/bmf

An automated microfluidic device for time-lapse imaging of mouse embryonic stem cells

Cite as: Biomicrofluidics 13, 054102 (2019); doi: 10.1063/1.5124057
Submitted: 10 August 2019 · Accepted: 20 August 2019 ·
Published Online: 17 September 2019

Adam F. Laing,[1] Venkat Tirumala,[2] Evan Hegarty,[1] Sudip Mondal,[1] Peisen Zhao,[3] William B. Hamilton,[4] Joshua M. Brickman,[4] and Adela Ben-Yakar[1,3,5,a)]

AFFILIATIONS

[1]Department of Mechanical Engineering, The University of Texas at Austin, 204 E. Dean Keeton St., Austin, Texas 78712, USA
[2]Department of Chemical Engineering, The University of Texas at Austin, 200 E. Dean Keeton St., Austin, Texas 78712, USA
[3]Department of Electrical and Computer Engineering, The University of Texas at Austin, 2501 Speedway, Austin, Texas 78712, USA
[4]The Novo Nordisk Foundation Center for Stem Cell Biology—DanStem, University of Copenhagen, 3B Blegdamsvej, DK-2200 Copenhagen N, Denmark
[5]Department of Biomedical Engineering, The University of Texas at Austin, 107 W. Dean Keeton St., Austin, Texas 78712, USA

[a)]**Author to whom correspondence should be addressed:** ben-yakar@mail.utexas.edu

ABSTRACT

Long-term, time-lapse imaging studies of embryonic stem cells (ESCs) require a controlled and stable culturing environment for high-resolution imaging. Microfluidics is well-suited for such studies, especially when the media composition needs to be rapidly and accurately altered without disrupting the imaging. Current studies in plates, which can only add molecules at the start of an experiment without any information on the levels of endogenous signaling before the exposure, are incompatible with continuous high-resolution imaging and cell-tracking. Here, we present a custom designed, fully automated microfluidic chip to overcome these challenges. A unique feature of our chip includes three-dimensional ports that can connect completely sealed on-chip valves for fluid control to individually addressable cell culture chambers with thin glass bottoms for high-resolution imaging. We developed a robust protocol for on-chip culturing of mouse ESCs for minimum of 3 days, to carry out experiments reliably and repeatedly. The on-chip ESC growth rate was similar to that on standard culture plates with same initial cell density. We tested the chips for high-resolution, time-lapse imaging of a sensitive reporter of ESC lineage priming, Nanog-GFP, and HHex-Venus with an H2B-mCherry nuclear marker for cell-tracking. Two color imaging of cells was possible over a 24-hr period while maintaining cell viability. Importantly, changing the media did not affect our ability to track individual cells. This system now enables long-term fluorescence imaging studies in a reliable and automated manner in a fully controlled microenvironment.

I. INTRODUCTION

Mouse embryonic stem cells (ESCs) are a highly useful experimental system for studying developmental biology and modeling disease.[1,2] They are genetically normal, immortal cell lines derived from the preimplantation embryo. Like the embryos from which they are derived, they are heterogeneous and dynamically recapitulate the earliest steps in differentiation. A huge variety of transgenic lines have been developed, including those with fluorescent markers showing the expression of genes-of-interest over time, capturing the heterogeneous nature of ESC culture and early differentiation. These types of cell lines are highly amenable to time-lapse imaging studies, allowing the behavior of individual cells to be measured in a quantitative and accurate manner over time.[3] This imaging can be combined with the perturbation of the cells with drugs, physical stimuli, or other techniques such as siRNA transfection to study the control networks behind these genes.[4,5] The highly quantitative nature of the data can be invaluable for modeling network control in both ESCs and other cell types.[6,7] However, carrying out these types of experiments using standard cell culture techniques remains technically highly challenging. Patterns of gene expression may be occurring over days and require maintaining a stable environment for imaging. Knowing the state of cells before and after a stimulus can explain

why some cells respond differently to others. The media must be continuously changed and drugs added and removed at desired time points during an experiment without disturbing imaging and tracking of individual cells. Automated microfluidic ESC cultures can be combined with time-lapse imaging to solve these problems.

Recent studies have shown the utility of microfluidic devices as a time-lapse imaging platform.[8–12] A versatile microfluidic cell culture chip was developed by Gomez-Sjoberg *et al.* and was used to grow a variety of cell types including mesenchymal stromal cells.[13] This device has also been used to study signaling dynamics in fibroblasts and macrophages.[14] However, cells were grown on a (polydimethylsiloxane) PDMS layer of substantial thickness over the glass, limiting the optical access for high-resolution imaging and high numerical aperture (NA) objectives. ESCs have also been grown in a chip directly on the glass to solve this problem, but this design uses complex fabrication and has no on-chip valves, thereby limiting their utility.[15]

A further obstacle to the more widespread uptake of the microfluidic technology to study ESC biology is a lack of published protocols for ESC culture in microfluidic conditions. Growing ESCs requires a specialized microenvironment that must be maintained to prevent ESC death and differentiation. Their culture has proved challenging to adapt to a microfluidic system and most time-lapse studies in chips to date use robust, immortalized lines such as HeLa.[9] Work has been done to optimize long-term ESC culture in microfluidics, albeit using a simple chip and feeder cells.[16] Other studies have grown both human and mouse ESCs in chips and used them to study pluripotency, differentiation, and even iPSC reprograming.[17–19] However, lack of a microfluidic platform specifically designed for high-resolution ESC time-lapse studies and the high difficulty of growing these cells in such systems have limited the adoption of this promising technology in the wider field.

We present here a versatile microfluidic chip, rationally designed for time-lapse studies of ESCs with precise and variable control of the microenvironment. We have also developed a robust and repeatable protocol for the long-term culture of ESCs in this chip with growth rates similar to those in macroscale conditions. This new protocol allows successful time-lapse studies of the cells over several days with media changes that does not disturb tracking of cells. The device integrates an upper valve layer and a lower culture layer with 3D ports, allowing both on-chip flow control and improving optical access to the cells. We demonstrate how this device can be used to conduct time-lapse imaging of a fluorescent ESC reporter line for extended periods.

II. METHODS

A. Device fabrication

Standard soft lithography methods[20] with slight alterations were used to fabricate our two-layer microfluidic devices. The top layer, containing flow channels and inputs, is shown in blue in Fig. 1(a). The bottom layer, containing cell culture chambers and valve actuation channels, is shown in red in Fig. 1(a). Photomasks printed on Mylar (Fineline Imaging) were used to create the photoresist patterns on a silicon wafer mold. The polydimethylsiloxane (PDMS, Sylgard 184, Dow Corning) microfluidic structures were made by combining molds from the two single-layer photoresist molds. First, we formed the top layer features by spin-coating positive photoresist (AZ50XT, Applied Electronic Materials) to a thickness of 55 μm onto a 4 in. silicon wafer.[21] Then, the mold is exposed through the first photomask using the mask aligner (MA6/BA6 Suss MicroTec), and the exposed photoresist is removed using a developer (AZ400 K 1:3, Applied Electronic Materials). Semicircular cross sections in the positive resist features were created with a reflow by ramping the temperature of the resist on a hotplate to 125 °C for 5 min allowing the resist to reach the glass transition temperature. The second mold was fabricated by spin-coating negative photoresist (SU-8 2075 Permanent Epoxy Negative Photoresist, MicroChem) to a thickness of 130 μm onto the second 4 in. silicon wafer and exposing the resist through the second photomask using the mask aligner. After both molds have been developed and hard baked, the surface of each mold was modified using trichlorosilane (SIT8174.0, Gelest Inc.) to make the molds hydrophobic which facilitates the release of the PDMS from the molds. All photoresist thicknesses were measured using a stylus profilometer (Dektak 6M, Veeco) to confirm the channel heights and the semicircular channel cross sections.

The PDMS top layer was fabricated by mixing the PDMS resin and the curing agent at a 10:1 ratio and poured the mixture onto the silanized positive photoresist mold to a height of 5 mm. The PDMS was baked at 80 °C for 45 min, peeled from the SU-8 mold, and holes for external connections were punched. The PDMS bottom layer was made by spin-coating the PDMS onto the SU-8 mold at 700 rpm for 33 s to achieve a height of 150 μm with an approximately 20 μm thick PDMS membrane covering the top of the valve features. The PDMS on the SU-8 mold was then partially cured in an oven at 80 °C for 8 min. The 5 mm-thick PDMS control layer was bonded to the partially cured imaging layer using a stereoscope for alignment. The two-layer PDMS chip was placed in an oven at 70 °C overnight. The two-layer PDMS device was then cut out and peeled from the mold, holes were punched for all remaining external connections and the 3D port locations, and the device was bonded to a large 180 μm thick cover using an oxygen plasma treatment (Nordson MARCH, CS-1701).

B. Cell culture

We used 2 different cell lines in this study: (1) HHex-Venus cells, which were described earlier[22] with a plasmid expressing a H2B-mCherry fusion cassette stably introduced for nuclear tracking. (2) Nanog-EGFP fusion reporter cells,[23] which were stably transfected with an expression cassette where an inducible cRaf-ErT2 fusion[24] is expressed with a H2B-mCherry nuclear label separated by a 2a peptide, allowing Erk induction and nuclear tracking from the same plasmid.

ESCs were maintained in standard culture conditions on 0.1% gelatin coated TC plasticware (Corning) in Glasgow Modified Eagle's Medium (GMEM, Sigma) containing 10% fetal calf serum, nonessential amino acids, L-glutamine, sodium pyruvate, 0.1 mM β-mercaptoethanol, and 1000 U/ml LIF. Cells were incubated at 37 °C in a humidified 5% CO_2 atmosphere. For fluorescence imaging experiments, media of the same composition were used with Fluorobrite (Sigma) replacing the GMEM.

For Calcein AM staining, cells were washed in the chips for 5 min with PBS and then 5 min with Calcein AM Green (Sigma) (2 μg/ml) at 120 μl/hr. Intracellular fluorescence was imaged after 10 min.

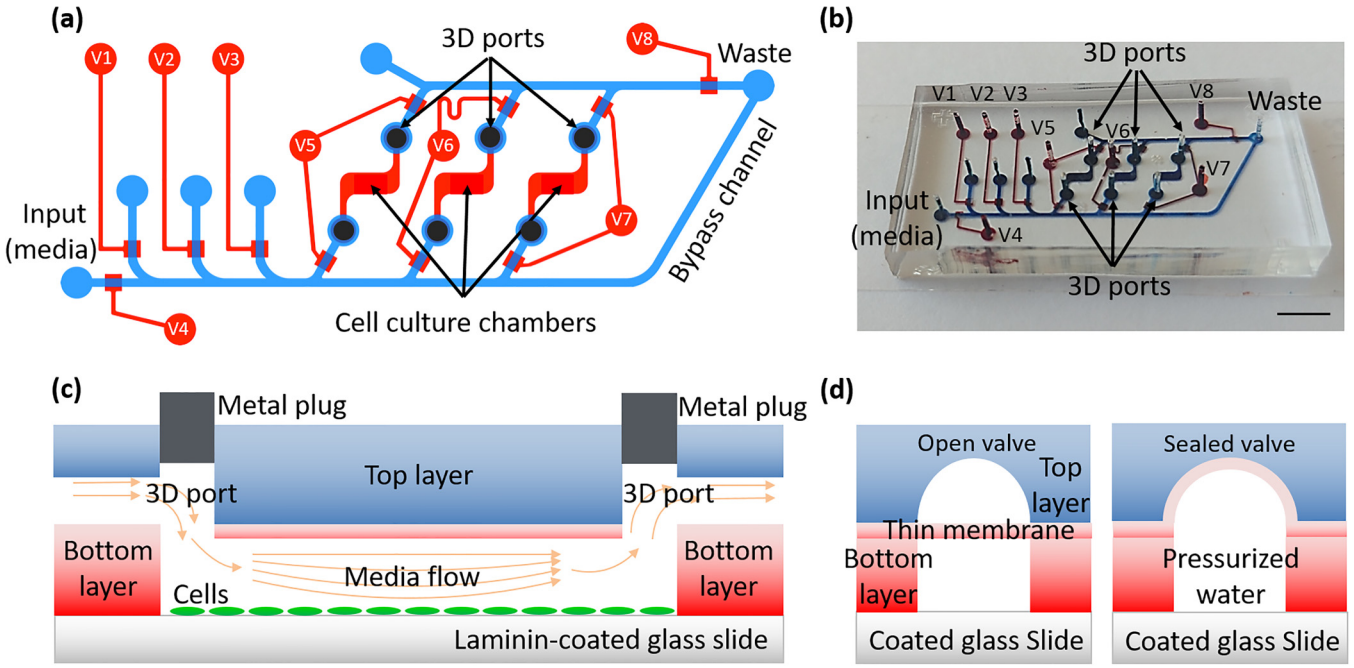

FIG. 1. Microfluidic chip for ESC culturing and time-lapse imaging. (a) Schematic of the device. Blue indicates the top layer with flow channels and inputs. Red is the bottom layer containing cell culture chambers and valve actuation channels. Valves V1–V4 control the main inputs for media and reagents. Valves V5–V7 are chamber isolation valves to allow separate feeding and perfusion regimes in each chamber. (b) Picture of the device showing flow channels/culture chambers (blue) and valves (red). The culture chambers are in the bottom layer but have the same color as the top layer since they are connected through the 3D ports. The scale bar represents 5 mm. (c) Cross-sectional schematic (along the flow direction) of the culture chambers in the device showing 2-layer structure and 3D ports connecting the top layer (blue) to the bottom layer (red) underneath the metal plug (gray). (d) The cross section (across the flow, flow is coming out of the page) of the completely-sealed valve geometry with open valve (0 psi) and sealed valve (25 psi) as the pressure is applied in the bottom valve chambers (V1–V8).

C. Device operation

On-chip valve operation was controlled using pressurized de-ionized water (DI) water lines connected to the actuation channels with 25 psi compressed air. These were operated by a solenoid valve system and a controller (ValveLink 8.1) controlled using a custom LabVIEW program.

Before use, the devices were washed thoroughly with ddH_2O for >5 days at approximately 4 ml/hr at 55 °C. They were then sterilized by autoclaving before use. This process ensured that any remaining contaminants in the exposed PDMS that were soluble in the aqueous media were removed. Chips were coated with 20 μg/ml laminin (Sigma) overnight at 4 °C. The chip was washed for more than 3 hr at 300 μl/hr with media before cell insertion to remove excess laminin and any remaining contaminants in the chip. The chip and all connected media reservoirs and tubing were initially pressurized with 5% CO_2 to 5 psi to remove any bubbles from the system. After washing, the flow rates in the chip were controlled by the withdrawal of a computer operated syringe pump (Braintree Scientific) that was attached to the chip waste outflow port. During experiments, the device was sealed into a stage top incubator (Bioscience Tools) in a humidified 5% CO_2 atmosphere at 37 °C to equilibrate the internal environmental conditions for the experiment.

For cell loading, a suspension of trypsinized and washed ESCs in media was injected into the chip through one of the input ports with a cell density calculated to load approximately 250 cells/mm^2. Chamber filling was observed and each chamber valve was sealed when the chambers were filled uniformly. Excess cells were then flushed from the loading channels, and the cells in the chambers were allowed to attach undisturbed for 2 hr before opening the chamber valves for the first media exchange. During the first media exchange (t = 0), the remaining unattached cells from the chambers were removed, and the density of attached cells was measured as the initial number of attached cells.

After the initial attachment period, media in each chamber was fully replaced every 2 hr considering the estimated time for media exhaustion in the microfluidic chambers. The duration of the media exchange and flow rates were tuned to replenish the entire chamber with nutrients while keeping the shear stress on the cells within the physiological limits as will be discussed in the section on Results. Media replenishment was fully automated and controlled by a custom LabVIEW program.

D. Time-lapse imaging

Time-lapse imaging experiments were performed on an inverted microscope (Olympus IX73) with an attached CCD

camera (Thorlabs 4070M-GE-TE) and high-precision motorized XYZ stage with a long range piezoelectric Z plate (ASI MS-2000). A custom-written LabVIEW program controlled image acquisition. This program also operated the motorized XYZ stage, motorized filter cube turret, and both white-light and fluorescent light source shutters to allow full automation of the imaging process. The system could be programed to scan several fields of views, covering the entire chamber at set intervals for bright-field imaging and for imaging the fluorescent proteins of interest. Before each scan, an autofocus routine adjusted the piezoelectric Z drive of the microscope stage using the chamber border as a focusing reference, to ensure that all images were captured in the same focal plane. Bright-field and fluorescence images of the microfluidic chambers were recorded using a 10× objective with a numerical aperture (NA) of 0.3 at multiple time points to count the total number of attached ESCs for characterizing the on-chip growth rates. To capture the changes in the gene expression of cells inside the chip, single-plane, fluorescence images of three fluorescence markers (Nanog-GFP, H2B-mCherry, and HHex-Venus) were also captured at high-resolution using a 40×, 0.95 NA objective.

E. Image analysis

We imaged the cells in the microfluidic chambers in two fields of views ($1.5 \times 1.5\,mm^2$) to capture the entirety of the chamber with sufficient overlap for proper stitching. We used a $1.2 \times 1\,mm^2$ area in the stitched images (at t = 0 h, right after the first media exchange), to manually count the initial density of attached cells per square millimeter of the chamber. The subsequent counting of the number of cells in fluorescence images at t = 16, 40, and 64 hr time points provided the cell growth rates for each chamber. Since the number of cells attached to the substrate varied for each chamber, we used the total number of cells at t = 16 hr to normalize the other two time points (t = 40 and 64 hr). Three researchers counted the cells independently, providing mean and standard deviations for each time point.

III. RESULTS

We combined several enabling features into one integrated microfluidic system to make it ideal for time-lapse imaging studies. Previous microfluidic culturing systems could only culture cells on the PDMS substrate when they incorporate microfluidic valves which required the users to culture their cells on top of a curved PDMS layer. In addition to the unfavorable substrate for cell culturing, the curved PDMS layer also degrades the ability to perform high-resolution imaging due to optical aberrations introduced by the curved PDMS structures in the previous designs. Taken as a whole, it is highly desired to culture the cells on the glass substrate, which allows the use of high-resolution, short working distance objectives while closely replicating the standard ESC culture conditions on a flat, rigid, protein coated surface. We, therefore, developed a novel microfluidic chip design [Figs. 1(a) and 1(b)], which incorporated three-dimensional (3D) ports connecting two separate layers: (1) the bottom layer that enables culturing of cells directly onto the glass, for the first time and (2) the top layer that incorporates fully sealing on-chip valves for flow control [Figs. 1(c) and 1(d)]. The curved cross section of the top layer allows complete sealing via pneumatically operated on-chip valves for flow control that can deliver various reagents on a timely and precise manner. This layer contains the input channels for reagents and cells. The bottom layer contains the cell culture chambers and valve actuation channels. The height of the chambers in this layer is approximately 130 μm.

The 3D ports, illustrated in Fig. 1(c), are fabricated by punching a hole through both PDMS layers, coupling the chambers in the top and bottom layers of PDMS. Then, a metal plug is inserted such that fluid can flow from the input channels in the top layer to the cell culture chambers in the bottom layer [Fig. 1(c)].[26] The main advantage of these 3D port configurations was that they enabled us to incorporate valves to completely seal the flow by deflecting the PDMS membrane on the curved channels of the top layer, while the cell culture chambers in the bottom layer remained in direct contact with the glass coverslip for the best optical access for high-resolution imaging [Fig. 1(d)]. The two layers were aligned and bonded, then punched through to make the inlet and outlet ports and the 3D ports connecting the layers. The finished cured device was plasma bonded to 180 μm thick glass slides and is shown in the macroscale view in Fig. 1(b).

The device contains 3 individually addressable culture chambers (2 mm long, 1 mm wide, and 130 μm tall, resulting in ~260 nl volume) to allow separate experiments to be carried out in each one. A bypass channel allows the channels to be washed out between the perfusion of different reagents and equalizes pressure between the inflow and outflow sides of the chip to prevent sudden flow when the chamber isolation valves are opened. Four input valves (V1–V4) are provided for media replenishment and experimental reagent perfusion.

Media in each chamber was fully replaced every 2 hr, based on the predicted minimum media exhaustion period of 2.1 hr. This period is proportional to the rate of media exhaustion in a macroscale 6-well plate culture where 2 ml media is generally renewed every 48 hr: 2 ml media/48 hr/10^6 cells (max population in the well) = 0.042 nl/hr/cell. Considering the maximum population in the chip is 3000 cells, the media is expected to deplete at a maximum rate of 125 nl/hr. Since the chamber volume is ~260 nl, the minimum chamber media exhaustion period is equal to ~2.1 hr.

To ensure equal perfusion rates in each chamber, we first flowed media through the bypass channel for 3 min to reach a steady-state flow rate of 120 μl/hr. Each chamber was then opened for 1 min, sequentially. At this rate, the average media residence time in the chamber volume was calculated to be ~8 s (260 nl/120 μl/hr flow rate = 7.8 s), ensuring complete media removal and replenishment in this period several times over. To account for the chamber geometry and to ensure that all areas were indeed flushed, specifically boundary layer region where cells are located, we measured the filling time across the chambers with fluorescein during perfusion. At the flow rate of 120 μl/hr, media were completely replaced across the entire chamber in less than 30 s [Video 1 in the supplementary material, Figs. 2(a) and 2(b)].

To verify that these perfusion rates did not introduce any disturbance on the cells, we estimated the shear stress. In a fully developed laminar flow in a rectangular geometry with 2D Poiseuille flow, the parabolic flow profile yields a shear stress of $\tau = \frac{6\mu Q}{h^2 w}$, where μ is the viscosity, Q is the flow rate, h is the chamber height, and w is the chamber width ($w > h$) at the bottom surface. In our

fluidic chamber with height 130 μm, width 1 mm, cell culture medium viscosity 0.78×10^{-3} N s/m^2, and flow rate 120 μl/hr, the cells attached to the bottom of the device are expected to experience a shear stress of <0.01 N/m^2. The value is well within the physiological limits, for example, hepatocytes experience a shear stress less than 0.2 N/m^2 *in vivo*, as summarized by Kim *et al.*[25] Following the above flow rate and media exchange estimates, we were able to standardize a culture condition to successfully grow ESCs in our novel microfluidic chip over 64 hr [Fig. 2(c)].

Mouse ESCs used in this study come from a line containing a sensitive fluorescent reporter, HHex-Venus.[22] HHex is a transcription factor expressed in the Primitive Endoderm (PrEn) lineage and this reporter is good readout of early and dynamic phases of PrEn differentiation. The HHex-Venus ESCs also contain an H2B-mCherry marker for cell nuclear tracking.[24] These features make this line an ideal candidate for time-lapse imaging on a microfluidic platform.

To enable such studies, we first tested the ability to grow ESCs for extended periods in our microfluidic device. ESCs were loaded at a density of around 250 cells/mm^2 and allowed to grow in the chips with periodic media replenishment. Previous studies have shown that periodic perfusion is preferable to continuous perfusion for microfluidic culture of ESCs as continuous flow induces differentiation.[16,18] Cells were imaged every 6 hr for 48 hr to qualitatively capture cell division and growth over time throughout the chamber as shown in Fig. 3(a). Video 2 in the supplementary material also shows cell growth in a representative experiment over a 3-day culture period. Cells grew evenly throughout the chambers and resembled those grown in macroscale culture.

To quantitatively analyze the growth rate of ESCs in our system, we counted the population over time. To minimize disturbance, cells were only imaged for a total of 64 hr every 24 hr after an initial period of 16 hr to allow for adhesion and adaption to the new environment. We used the H2B-mCherry nuclear marker to facilitate manual cell counting and calculate cell growth over time. In a whole-chip experiment, we measured the cell growth rates in all three chambers of the same chip [Fig. 3(b)]. While the density of cells loaded to the chip was ~250 cells/mm^2, the density of the attached cells to the surface of each chamber after the initial 2 hr attachment period and perfusion varied between 127 and 208 cells/mm^2. The growth rates followed a consistent trend and scaled in proportion with the initial cell density. The average number of cells increased by 2.49 ± 0.67 and 5.53 ± 0.83 (mean ± standard deviation) at t = 40 and 64 hr as compared to the initial cell counts at t = 16 hr [Fig. 3(c)].

Additional cell growth rate measurements in four separate chip experiments over 64 hr time in Chamber A showed a reproducible trend, where cells could approximately double every 24 hr [Fig. 3(d)]. The measured average number of cells increased by 2.48 ± 0.89 and 2.23 ± 0.97 within the time frames of 16–40 hr and 40–64 hr, respectively [Fig. 3(e)].

In another set of full chip experiment, we observed that the initial attached cell density did not have an effect on the growth rate within the first 16 hr. Although the average 16 hr cell growth rate

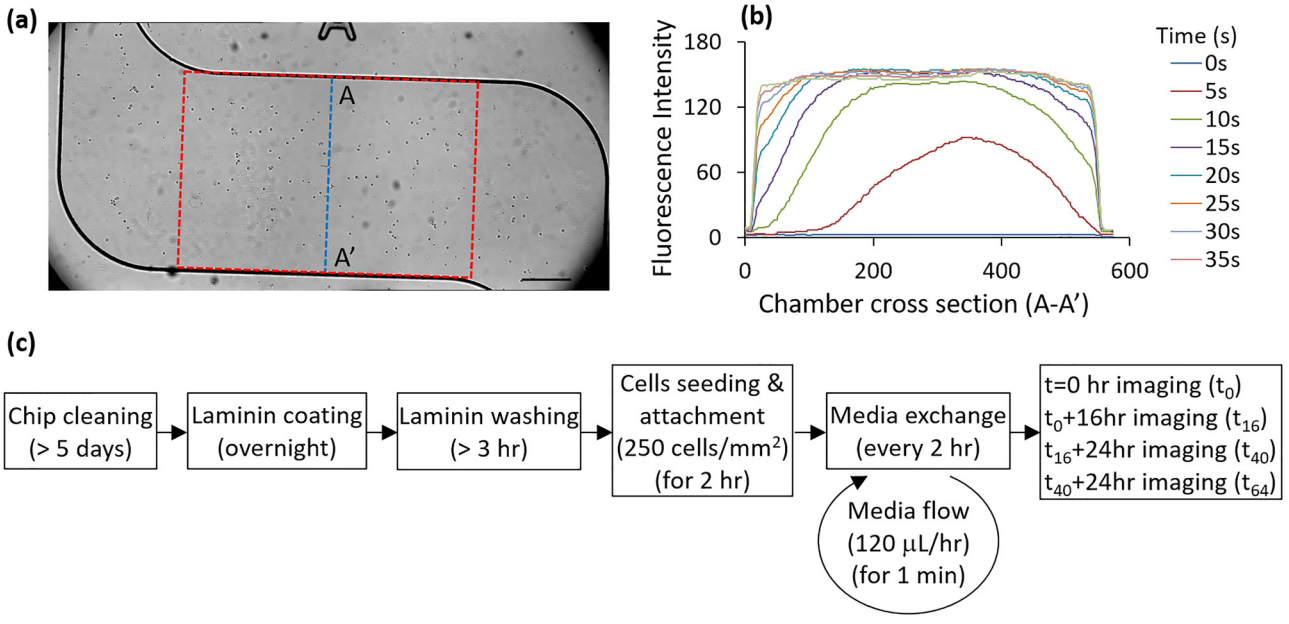

FIG. 2. On-chip imaging and long-term culturing protocols for time-lapse studies. (a) The bright-field image of an ESC culture chamber. The rectangular box (red) is the portion of the culture chamber used to count the total number of cells and estimate cell growth rates. The blue line (AA′) along the chamber width is used to analyze the fluorescence signal from the fluorescein and characterize the transients during buffer exchanges. The scale bar represents 250 μm. (b) The intensity increase of fluorescein as it is filling one of the microfluidic culture chambers along AA′ across the chamber width when perfused at a flow rate of 120 μL/hr. (c) Flow chart of the chip preparation and media exchange for long-term culturing and fluorescence time-lapse imaging at 0 (t_0), 16 (t_{16}), 40 (t_{40}), and 64 hr (t_{64}) time points. To minimize disturbance during cell proliferation measurements, we imaged cells with H2B-mCherry nuclear marker every 24 hr after initial attachment period of 16 hr.

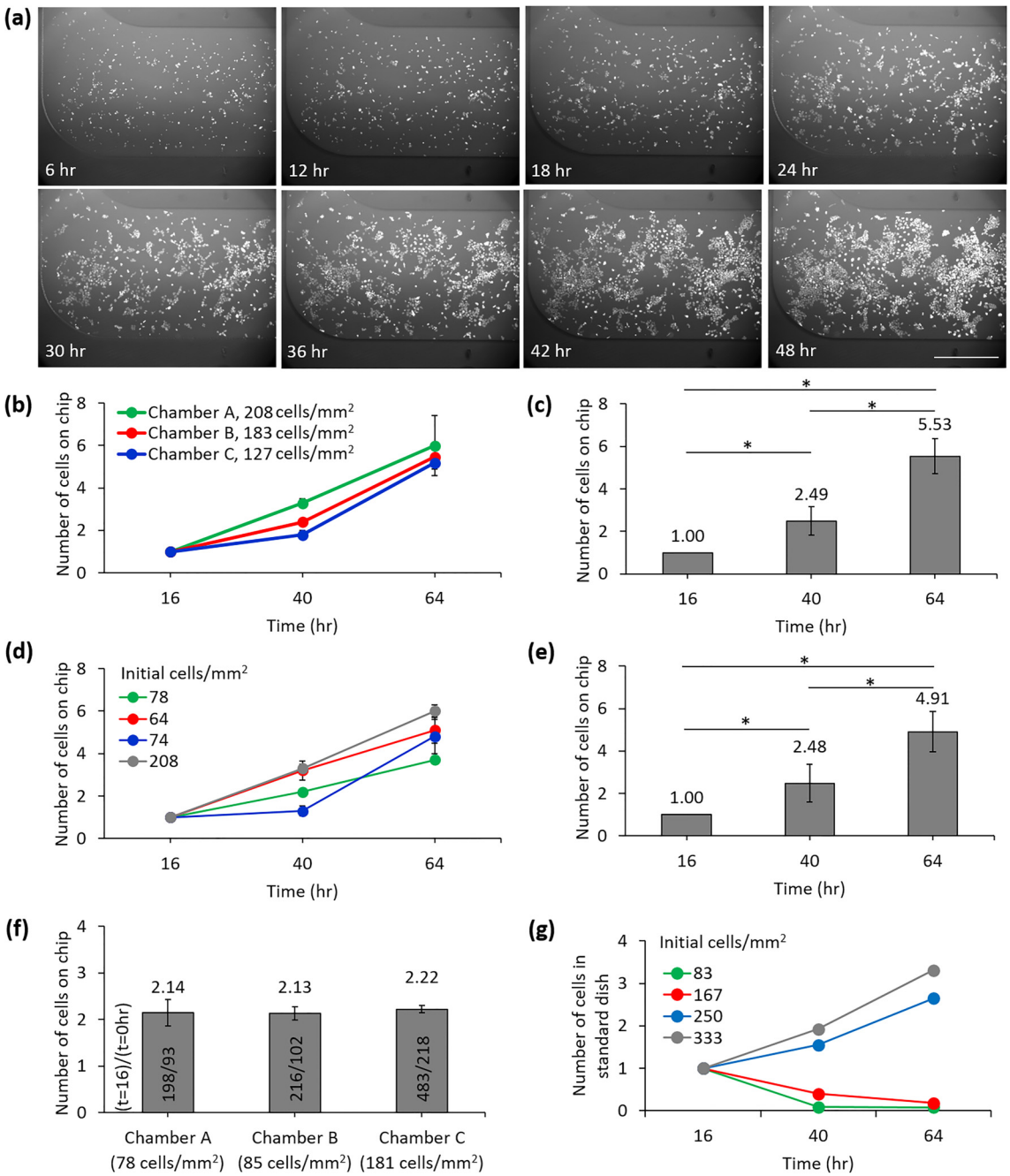

FIG. 3. Growth rate of ESCs cultured in the microfluidic chip. (a) Examples of time-lapse fluorescence images of ESCs growing over 48 hr as taken every 6 hr. Each spot indicates a single ESC nucleus labeled with the H2B-mCherry marker. The scale bar is 500 μm. (b) Number of ESCs in all three chambers (Chambers A, B, and C) of a single microfluidic chip at different time points as normalized by the number of cells at 16 hr time point. The slope of each line represents the growth rate. The initial density of cells is calculated from the total number of attached cells after 2 hr of incubation followed by a wash step. Cells were counted every 24 hr after an initial 16 hr period. (c) The average number of cells from all three different chambers shown in (b) at different time points. Data represented as mean ± standard deviation. The significance is calculated with Student *t* test with p-value <0.001 (*). (d) Number of ESCs in Chamber A of four different chips at different time points as normalized by the number of cells at t = 16 hr. (e) The average of cell counts, represented as mean ± standard deviation. The significance is calculated with Student *t* test with p-value <0.001 (*). (f) Additional data showing the initial 16-hr growth rates of cells in all three chambers from a single microfluidic chip experiment. (g) Number of ESCs in standard macroscale culture conditions (laminin coated dishes) over time.

was slightly higher for Chamber C with higher initial cell density at t = 0 hr, it was not statistically significant as compared to Chambers A and B that had less initial cell densities at t = 0 hr [Fig. 3(f)].

To ensure that cells in our microfluidics system were growing in a similar rate to those in standard macro culture conditions, we also measured the growth rate of ESCs grown in laminin coated glass bottom dishes at varying initial cell densities [Fig. 3(g)]. At the cell seeding density of $\geq$250 cells/mm^2, the cells on glass dishes multiplied by 1.56–1.70 between the time frames of 16–40 hr and 40–64 hr, respectively. While cells at low initial densities have low viability in macroculture conditions, those ESCs plated at similar or higher densities in the chips expanded well. We can then conclude

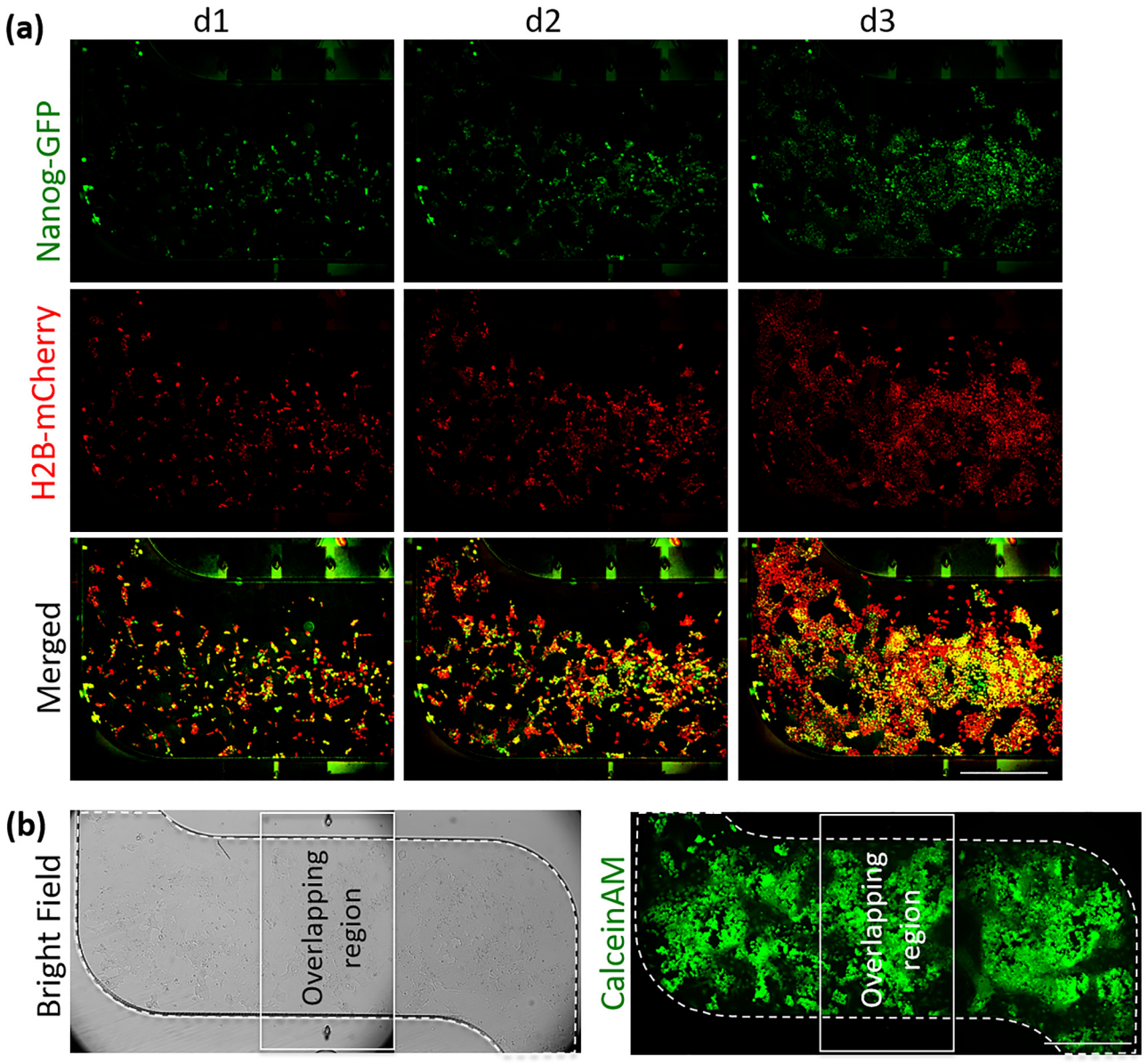

FIG. 4. Viability and pluripotency studies of ESCs grown in a microfluidic chip. (a) Expression of Nanog in ESCs as shown by a Nanog-GFP reporter line. H2B-mCherry shows cell nuclei. Merged images are color-balance adjusted to show the overlap of mCherry/GFP in yellow. Images were taken after 1, 2, and 3 days of culturing in chip after an initial 16 hr of the initial adaptation period. (b) Bright-field and Calcein AM staining images showing viable ESCs after 3 days culture in a chip from another independent growth experiment using the microfluidic chip. The white dashed boundary represents the microfluidic chamber with cells. The white rectangle indicates the overlapping portion of the chamber between two imaging field of views. The scale bars are 500 μm.

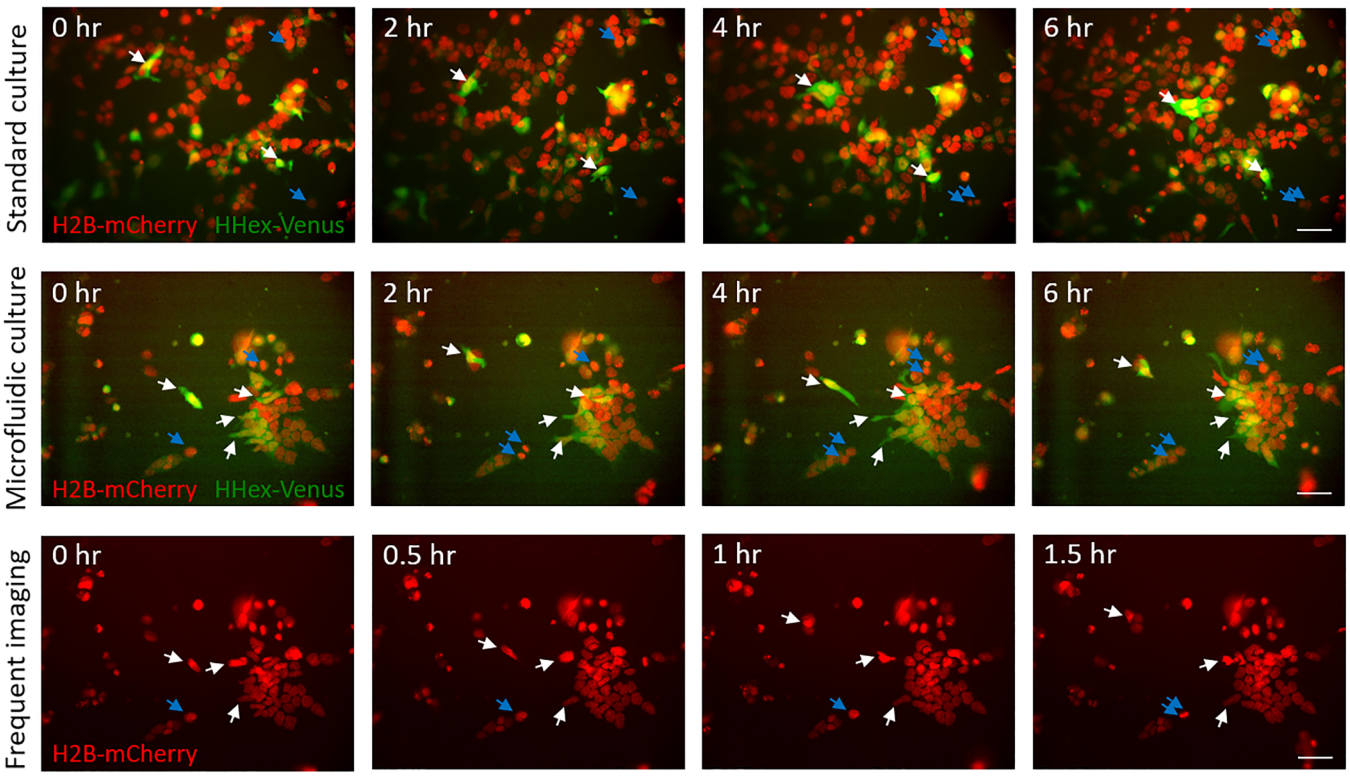

FIG. 5. High-resolution fluorescence images of cell migration of the cells growing inside the standard culture dish and microfluidic chip as acquired using a 40×, 0.95NA objective. The fluorescence images for H2B-mCherry (nuclei) and HHex-Venus (PrEn lineage) were acquired every 30 min and 2 hr, respectively, and colocalized in the figures. White arrows indicate the migrating cells. Blue arrows indicate the cell division processes. The bottom panel represents frequent images of the H2B-mCherry marked cells, showing cell migration (white arrows) and chromosome rearrangement during the cell division process (blue arrows). Scale bar is 50 μm.

that compared to standard growth conditions on plates, cells in our chip have a similar growth rate even when fewer cells are attached at the bottom surface of the growth chamber.

As ESCs are prone to spontaneous differentiation in substandard culture environments, we also looked at levels of a pluripotency marker, Nanog, within cells cultured in the microfluidic chip.[27] In additional sets of experiments, ESCs expressing a Nanog-GFP reporter were grown on the chips and imaged after 3 days. We found that the cells continued to express this marker in a heterogeneous pattern as expected [Fig. 4(a)]. We also confirmed that cells growing in the chips were alive and metabolically active using a Calcein AM stain. After 3-day culturing, virtually all cells were visible and stained positive for the live cell marker [Fig. 4(b)]. These experiments confirmed that our on-chip culturing protocols could maintain healthy cultures of ESC over extended periods within the entire microfluidic chamber. We did not observe any zonation, namely, regions with low/poor growth rates.

We also demonstrated long-term time-lapse imaging of fluorescent reporters in our chips and compared it to those grown in standard culture conditions. HHex-Venus cells were cultured on the chips as before, and after an initial 16 hr cultural adaptation period, time-lapse imaging of Venus and H2B-mCherry was carried out for 24 hr (Videos 3 and 4 in the supplementary material). mCherry images were acquired every 30 min to allow identification and tracking of individual cells throughout migration and cell division events (Fig. 5 and Video 3 in the supplementary material). Venus is much dimmer than H2B-mCherry due to low levels of HHex expression in ESCs and, therefore, imaging required longer exposure time and use of a high NA objective (0.95NA, 40×). Therefore, Venus was imaged every 2 hr which still provided a high enough temporal resolution to capture gene expression changes at the single-cell level while minimizing potential phototoxicity. The morphology of the cells growing in the microfluidic devices was similar to the morphology of cells growing in the standard culture conditions on dishes. After a 24 hr period, imaged cells did not show increased signs of lysis compared to those in an unexposed area, showing that phototoxicity was not an issue under the imaging conditions used.

IV. CONCLUSIONS

We have constructed a new microfluidic device, designed from the ground up to provide a solution to the technical challenges of performing long-term culturing of ESCs for high-resolution, time-lapse imaging. Unlike traditional methods of time-lapse imaging in

plates, this device provides a stable environment for cells over long periods with regular automated replenishment of media. The microenvironment can also be precisely varied over time by perfusion media containing drugs or other small molecules without interrupting sensitive imaging.

Our microfluidic device is a marked improvement on previously published chips in several ways. It combines 3D ports connecting 2 layers: one with completely sealed valves and a separate culture/imaging layer that can be bonded onto a thin glass substrate enabling high-resolution imaging. Growing cells directly on the thin glass instead of a PDMS layer as previously done allows the use of short working distance/large NA objectives which are vital for performing high-resolution microscopy, or imaging low brightness fluorescent proteins as shown in this study. Although ESCs have previously been grown inside microfluidic chips directly on the glass substrate to improve the imaging constraints, such devices use complex fabrication and have no full sealing on-chip valves.[28] Such devices are limited in their utility for complex culture conditions, requiring multiple chemical exposures and controlled exposure times. Unlike these other published devices, the fabrication methods used here are standard, and the chips do not require complicated support apparatus.

Importantly, we have developed a robust protocol for culturing ESCs within the chip, with cell density doubling every 24 hr, and maintaining cell viability and pluripotent phenotypes over time. This protocol allows repeated experiments to be carried out reliably. Finally, we have developed and integrated a time-lapse imaging system with our devices. High-resolution time-lapse imaging of ESCs growing inside the microfluidic chamber show similar cell motility and dynamics as found in conventional cultures. The platform enabled measurement of gene expression at the single-cell level with high spatial and temporal resolutions. We have limited our current study to 3 days, to eliminate the adverse effects of an over-confluent cell population. Although cells can continue to grow beyond 3 days, abnormal results and cell differentiation can result due to over-confluent cells.[29] This system is easily adaptable with commercially available imaging systems, and we have shown that it can be used to reliably image ESCs growing in the devices for any period of time.

SUPPLEMENTARY MATERIAL

See the supplementary material for videos of perfusion conditions and time-lapse imaging of cell growth and dynamics on the microfluidic chip.

ACKNOWLEDGMENTS

This work was funded by the Human Frontier Science Program (No. RGP0008/2012) and partially funded by NIH Director's Transformative Award from the National Institute on Aging (No. NIH/NIA R01 AG041135). Device fabrication was carried out at the Center for Nano and Molecular Science, UT Austin. Nanog:EGFP reporter cells were a kind gift from Matt Thomson at UCSF.

REFERENCES

[1]M. J. Evans and M. H. Kaufman, "Establishment in culture of pluripotential cells from mouse embryos," Nature **292**(5819), 154–156 (1981).
[2]G. Martello and A. Smith, "The nature of embryonic stem cells," Annu. Rev. Cell Dev. Biol. **30**, 647–675 (2014).
[3]T. Schroeder, "Long-term single-cell imaging of mammalian stem cells," Nat. Methods **8**(4 Suppl.), S30–S35 (2011).
[4]M. Thomson *et al.*, "Pluripotency factors in embryonic stem cells regulate differentiation into germ layers," Cell **145**(6), 875–889 (2011).
[5]E. Abranches *et al.*, "Stochastic NANOG fluctuations allow mouse embryonic stem cells to explore pluripotency," Development **141**(14), 2770–2779 (2014).
[6]C. V. Harper *et al.*, "Dynamic analysis of stochastic transcription cycles," PLoS Biol. **9**(4), e1000607 (2011).
[7]C. Schroter *et al.*, "FGF/MAPK signaling sets the switching threshold of a bistable circuit controlling cell fate decisions in embryonic stem cells," Development **142**(24), 4205–4216 (2015).
[8]D. M. Thompson *et al.*, "Dynamic gene expression profiling using a microfabricated living cell array," Anal. Chem. **76**(14), 4098–4103 (2004).
[9]D. R. Albrecht *et al.*, "Microfluidics-integrated time-lapse imaging for analysis of cellular dynamics," Integr. Biol. **2**(5–6), 278–287 (2010).
[10]J. Tam *et al.*, "A microfluidic platform for correlative live-cell and super-resolution microscopy," PLoS One **9**(12), e115512 (2014).
[11]A. S. Hansen, N. Hao, and E. K. O'Shea, "High-throughput microfluidics to control and measure signaling dynamics in single yeast cells," Nat. Protoc. **10**(8), 1181–1197 (2015).
[12]T. Chen *et al.*, "A drug-compatible and temperature-controlled microfluidic device for live-cell imaging," Open Biol. **6**(8) 160156 (2016).
[13]R. Gomez-Sjoberg *et al.*, "Versatile, fully automated, microfluidic cell culture system," Anal. Chem. **79**(22), 8557–8563 (2007).
[14]R. A. Kellogg *et al.*, "High-throughput microfluidic single-cell analysis pipeline for studies of signaling dynamics," Nat. Protoc. **9**(7), 1713–1726 (2014).
[15]L. Kim *et al.*, "Microfluidic arrays for logarithmically perfused embryonic stem cell culture," Lab Chip **6**(3), 394–406 (2006).
[16]S. Giulitti *et al.*, "Optimal periodic perfusion strategy for robust long-term microfluidic cell culture," Lab Chip **13**(22), 4430–4441 (2013).
[17]Y. S. Zhang *et al.*, "Patterning pluripotency in embryonic stem cells," Stem Cells **31**(9), 1806–1815 (2013).
[18]L. M. Przybyla and J. Voldman, "Attenuation of extrinsic signaling reveals the importance of matrix remodeling on maintenance of embryonic stem cell self-renewal," Proc. Natl. Acad. Sci. U.S.A. **109**(3), 835–840 (2012).
[19]C. Luni *et al.*, "High-efficiency cellular reprogramming with microfluidics," Nat. Methods **13**(5), 446–452 (2016).
[20]M. A. Unger *et al.*, "Monolithic microfabricated valves and pumps by multilayer soft lithography," Science **288**(5463), 113–116 (2000).
[21]S. K. Gokce *et al.*, "A multi-trap microfluidic chip enabling longitudinal studies of nerve regeneration in *Caenorhabditis elegans*," Sci. Rep. **7**(1), 9837 (2017).
[22]M. A. Canham *et al.*, "Functional heterogeneity of embryonic stem cells revealed through translational amplification of an early endodermal transcript," PLoS Biol. **8**(5), e1000379 (2010).
[23]C. Sokolik *et al.*, "Transcription factor competition allows embryonic stem cells to distinguish authentic signals from noise," Cell Syst. **1**(2), 117–129 (2015).
[24]W. B. Hamilton and J. M. Brickman, "Erk signaling suppresses embryonic stem cell self-renewal to specify endoderm," Cell Rep. **9**(6), 2056–2070 (2014).
[25]L. Kim *et al.*, "A practical guide to microfluidic perfusion culture of adherent mammalian cells," Lab Chip **7**(6), 681–694 (2007).
[26]S. K. Gökçe *et al.*, "A fully automated microfluidic femtosecond laser axotomy platform for nerve regeneration studies in *C. elegans*," PLoS One **9**(12), e113917 (2014).
[27]I. Chambers *et al.*, "Nanog safeguards pluripotency and mediates germline development," Nature **450**(7173), 1230–1234 (2007).
[28]A. J. Kaestli, M. Junkin, and S. Tay, "Integrated platform for cell culture and dynamic quantification of cell secretion," Lab Chip **17**(23), 4124–4133 (2017).
[29]M. Belacel-Ouari *et al.*, "Influence of cell confluence on the cAMP signalling pathway in vascular smooth muscle cells," Cell Signal. **35**, 118–128 (2017).